A selective muscle fatigue management approach to ergonomic human-robot co-manipulation

Peternel, Luka; Fang, Cheng; Tsagarakis, Nikos; Ajoudani, Arash

DOI
10.1016/j.rcim.2019.01.013

Publication date
2019

Document Version
Accepted author manuscript

Published in
Robotics and Computer-Integrated Manufacturing

Available online at www.sciencedirect.com

ScienceDirect

Robotics and Computer-Integrated Manufacturing 00 (2019) 1–17

RCIM

A Selective Muscle Fatigue Management Approach to Ergonomic Human-Robot Co-Manipulation

Luka Peternel[a,b,*], Cheng Fang[c], Nikos Tsagarakis[c], Arash Ajoudani[a]

[a] *HRI[2] Lab, Department of Advanced Robotics, Istituto Italiano di Tecnologia, Via Morego 30, 16163 Genoa, Italy*
[b] *Department of Cognitive Robotics, Delft University of Technology, Mekelweg 2, 2628 CD Delft, The Netherlands*
[c] *HHCM Lab, Department of Advanced Robotics, Istituto Italiano di Tecnologia, Via Morego 30, 16163 Genoa, Italy*

Abstract

In this paper, we propose a method for selective monitoring and management of human muscle fatigue in human-robot co-manipulation scenarios. The proposed approach uses a machine learning technique to learn the complex relationship between individual human muscle forces, arm configuration and arm endpoint force that are provided by a sophisticated offline musculoskeletal model. The estimated muscle forces are used in the fatigue model to estimate the individual muscle fatigue levels online. Two fatigue management protocols are proposed that enable the robot to handle and reduce the human fatigue by altering the configuration of task execution. The first protocol uses optimisation technique to find the optimal position for task execution, where the fatigue-related endurance time can be maximised. The second protocol divides the arm muscles into groups and then alters the direction of endpoint force so that the fatigued muscle group can relax and the relaxed muscle group becomes active. The proposed method has a potential to enable the robot to facilitate safer and more ergonomic working conditions for the human coworker. The main advantage of this approach is that it can operate online, and that all the measurements can be performed by the robot sensory system, which can significantly increase the applicability in real world scenarios. To validate the proposed method, we performed multiple experiments with two collaborative tasks (polishing and drilling) under different conditions.

Keywords:
Physical Human-Robot Collaboration, Muscle Fatigue, Muscle Force Estimation, Machine Learning

1. Introduction

The recent trend in robotics puts a considerable stress on including humans into the industrial production process in an attempt to use the human's superior flexibility/adaptability and retain the jobs for the human workers. The aim is to move the robots out of the cages and make them collaborate with the human workers in various complex tasks. In this direction, the amount of research related to human-robot collaboration (HRC) has been rapidly increasing in the past years [1], especially for manufacturing tasks [2, 3].

One of the key problems of HRC is to make humans and robots be aware of each other's intentions, and intelligently collaborate to achieve manufacturing objectives. To solve this problem, the collaborative robots have been equipped with various sensory systems and processing modules to facilitate the interpretation of the human's intentions and states [4, 5, 6, 7, 8, 9, 10], and to generate robot behaviours to react appropriately and accordingly [4, 11, 12, 2, 10, 13]. Common sensory systems to detect the human function and intention are based on force measurements [4, 5, 6, 14, 7, 8, 9], visual feedback [12], and language command recognition [15]. These systems can be

*Corresponding author (email: l.peternel@tudelft.nl)

mounted on the robot and pose no discomfort to the human coworker. On the other hand, some additional sensory systems that are attached to the human coworker, such as electromyography (EMG) [10], or electroencephalography (EEG) [16], can greatly enhance the robot's awareness of human intention and states. However, this can come at the price of increased cost and the imposed discomfort to the human coworker.

Safety and well-being of workers during human-robot collaboration is a crucial issue in industrial settings [17, 18]. Some of the above-mentioned sensory modalities can also be used to estimate human performance degradation during HRC, which is is usually caused by excessive levels of physical or cognitive fatigue. This aspect is particularly important to ensure a favourable condition of human workers. For example, excessive cognitive fatigue may result in human making more mistakes and hindering the production process. In another instance, excessive physical fatigue may result in musculoskeletal disorders that require long-term treatments and inevitable absence of the worker from the production process.

Several existing methods proposed to analyse and solve the fatigue-related issues from the physical perspective in HRC. The robot can help to reduce the effect of an external load on human joints (e.g. see our previous work in this direction [13, 19]). Alternatively, the robot can monitor and manage the amount of fatigue generated by active exertion of muscle forces [20, 21]. This paper aims to provide novel effective tools and solutions to address the latter.

A simple and effective tool to analyse the muscle fatigue is to observe the changes of the EMG signal in frequency domain. It has been shown that the mean amplitude of EMG increases and mean frequency of the spectrum decreases with the muscle fatigue [22]. While this approach works well for a constant muscle effort, it may not be reliable for dynamical tasks where the muscle effort is changing. To resolve this issue, model-based techniques that are based on the EMG [21] or force [23] measurements have been proposed instead.

The authors in [20] measured the human arm endpoint force and used the fatigue model proposed in [23] to monitor the human fatigue. Since the force was only measured at the endpoint and the method offers no relation between endpoint force and individual muscle forces, the individual muscle fatigue cannot be estimated. The human joints are actuated by many muscles that have a combined contribution to the endpoint force. If we wish to estimate individual muscle fatigue levels, the muscle forces should therefore be estimated individually.

To estimate the individual muscle forces, one can use complex models of musculoskeletal dynamics [24] and systems [25, 26] from the literature. However, the underlying complexity of such models and reliance on off-line optimisation techniques limits their application to offline calculation and may therefore not be suitable for HRC, where online adaptation is a crucial requirement. On the other hand, although direct muscle activity measurements by EMG [21] enable precise selection and monitoring of individual muscles, the application of EMG in industrial and other real-world scenarios may be impractical. In addition, some muscles lay under the surface and cannot be reached by the surface EMG.

To solve the limitations of the above-mentioned methods for human muscle fatigue monitoring in HRC, we propose a novel method that enables online estimation of individual muscle forces in the human arm. We utilise a machine learning technique to learn the mapping between the arm endpoint force, arm configuration and muscle forces. The relationship between these variables is first obtained from an accurate and complex musculoskeletal model in an offline calibration stage. The obtained mapping is then used in an online stage by the collaborative robot to selectively estimate the human muscle fatigue and then adjust its behaviour in an attempt to reduce it. To this end, the proposed method includes a novel fatigue management system that involves two main management protocols. The first protocol is based on an optimisation approach that allows the robot to find the optimal endpoint position for task execution, where the fatigue-related endurance time is maximised. The second protocol enables the robot to change the task execution configuration to selectively offload the human coworker's muscles, which are currently under a considerable fatigue, by delegating the task load to the relaxed muscles instead.

The main contributions of the presented research are: i) an approach to use machine learning to make complex offline muscle force model work online in real-time, ii) a multi-protocol fatigue management method that enables the robot to change the working configuration of the task in order to alleviate the fatigue of the specific tired muscles of collaborating human.

The proposed method is experimentally validated on a human-robot co-manipulation setup using KUKA Lightweight Robot arm. We considered two common industrial tasks. In the first task, the human is asked to polish a surface of an object that is held and manipulated by the collaborative robot. In the second task, the human is asked to drill into an object that is held and manipulated by the robot.

A preliminary version of the proposed fatigue management framework was presented at 2018 IEEE/RSJ Interna-

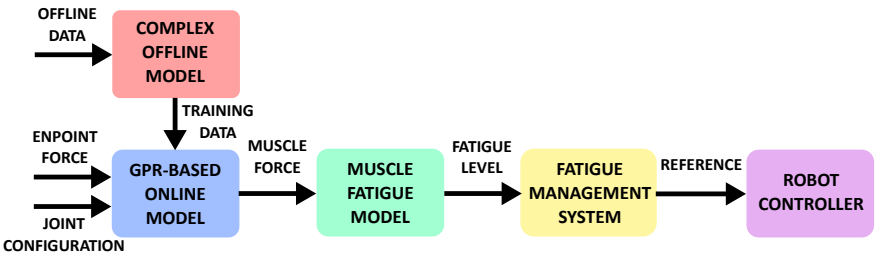

Figure 1: Block scheme of the proposed method. A complex biomechanical model is used in an offline calibration process to obtain the training data for *Gaussian Process Regression* (GPR). The online GPR-based model is then used to predict the individual muscle fatigue during the human-robot co-manipulation task. The fatigue management system then changes the robot behaviour in order to either maximise the fatigue-related endurance time or selectively offload the tired muscles and put more load on the ones with lower fatigue levels.

tional Conference on Intelligent Robots and Systems [27]. This paper extends the preliminary study in several aspects. The methodology of fatigue management system is significantly extended. The online management protocol is upgraded with a method that can group muscle based on the endpoint force direction. In addition to the online method, we add a planning-based protocol that can optimise the endurance time of endpoint force production by considering muscle fatigue model. To strengthen the validation of the proposed approach, an additional experimental task (i.e., drilling task in addition to polishing task) and additional experiments and results and are included.

2. Methods

The block scheme in Fig. 1 illustrates the proposed selective muscle fatigue management approach. In the offline stage we obtained the model that the robot can use to estimate the muscle forces in the online stage. During a preliminary calibration experiment we collected a variation of human arm configurations and endpoint forces in different conditions. We then used the collected data in conjunction with a complex human arm musculoskeletal model and optimisation process to estimate individual muscle forces for different measured conditions. The *Gaussian Process Regression* (GPR) was employed to learn the relationship between the given configuration and endpoint force inputs and muscle force outputs.

We then used the obtained function encoded with GPR in the control of human-robot co-manipulation. The control method used the interaction force (measured by a force sensor at the robot end-effector) and human arm configuration (measured by a motion capture system) as GPR inputs to estimate the muscle forces at each sample time. The estimated muscle forces were then used in a modified muscle fatigue model that was based on the model we recently proposed in [21].

To enable the robot to selectively manage the fatigue of different muscles, we developed a method with two management protocols, each of them dealing with two most common constraints (i.e., endpoint orientation and position constraints). First protocol finds the optimal working position within an orientation constraint in Cartesian space through the optimisation process, where the fatigue-related endurance time of the human arm is maximised. The second protocol changes the task execution configuration within a position constraint in Cartesian space in a way that offloads the fatigued muscles and puts stress on the less fatigued muscles. The robot does this by making the human change the working conditions in a way that the fatigued muscle does not need to contribute to the endpoint force required for the task production (e.g., the orientation of an object is changed so that the drilling/polishing force must be produced in a different direction).

2.1. Human Arm Model

We can define a quasi-static relation between the human arm joint torques and endpoint force as

$$\boldsymbol{\tau}_h = \boldsymbol{J}_h^T(\boldsymbol{q}_h)\boldsymbol{f} + \boldsymbol{g}_h(\boldsymbol{q}_h), \tag{1}$$

where $\boldsymbol{\tau}_h$ is joint torque vector of the human arm, $\boldsymbol{f}$ is endpoint force vector, $\boldsymbol{J}_h$ is geometric Jacobian matrix of the human arm, $\boldsymbol{q}_h$ is joint angle vector and $\boldsymbol{g}_h$ is the gravity torque vector of the arm.

The muscles in the human arm produce the joint torques by exerting forces as

$$\boldsymbol{\tau}_h = \boldsymbol{J}_m^T(\boldsymbol{q}_h)\boldsymbol{f}_m, \tag{2}$$

where $\boldsymbol{f}_m$ is muscle force vector and $\boldsymbol{J}_m$ is muscle Jacobian matrix containing moment arms of different muscles. Each specific joint has at least one pair of antagonistically coupled muscles that pull it in two opposite directions. Typically, more than one pair of antagonistic muscles are usually acting on a single joint [28].

By combining (1) and (2), we derive a relation between the human arm muscle forces and the endpoint force

$$\boldsymbol{f}_m = \boldsymbol{J}_m^{-T}(\boldsymbol{q}_h)\Big(\boldsymbol{J}_h^T(\boldsymbol{q}_h)\boldsymbol{f} + \boldsymbol{g}_h(\boldsymbol{q}_h)\Big). \tag{3}$$

The current muscle forces $\boldsymbol{f}_m$ in the arm could theoretically be calculated by given measured endpoint interaction force $\boldsymbol{f}$ and arm configuration $\boldsymbol{q}_h$. However, the transformation $\boldsymbol{J}_m^{-T}$ has a redundancy, if more antagonistic pairs of muscles are acting on a single joint. In such case, (3) does not have an unique solution. For example, many possible combinations of forces from different muscles that act on a specific joint can produce the same joint torque. Among these possible mathematical solutions there are also some that prescribe negative muscle forces, which is physiologically impossible since muscles can act only in one direction (i.e. can only pull and cannot push).

Researchers commonly apply optimisation techniques to resolve the redundancy of mapping from $\boldsymbol{\tau}_h$ to $\boldsymbol{f}_m$ in (3). Literature mainly reports three different methods for estimating muscle forces: *Static Optimization* (SO) [29], *Computed Muscle Control* (CMC) [30] and *Neuromusculoskeletal Tracking* (NMT) [31]. SO distributes relevant muscle forces according to the net moment applied at each joint by optimising a specified performance criterion without considering any human arm dynamics behaviour. On the other hand, CMC and NMT resolve the muscle force distribution issue by involving and integrating muscle activation dynamics, muscle contraction dynamics and body-segmental dynamics simultaneously. In addition, CMC and NMT differ in the effective time span of the optimisation. Specifically, the optimisation in CMC works locally at each time instant, whereas NMT attempts to optimise a time-dependent performance criterion globally over the entire human motion (e.g., minimising metabolic energy consumption [32]).

Comparisons between these three optimisation methods were conducted in previous research and convincing similarity of the muscle force estimates were observed and manifested in most of cases excluding highly dynamic human motions, such as jumping and sprint running [33, 34]. These previous studies suggest that the incorporation of muscle activation and contraction dynamics and/or time-dependent performance criterion do not significantly influence the muscle force estimation in static or quasi-static applications (e.g., HRC tasks like polishing, drilling, etc.). For this reason, SO is a more appealing method for estimating muscle forces because it is computationally more robust and efficient, and was therefore employed in this work.

The optimisation problem of distributing muscle forces in SO can be formulated as

$$\begin{aligned} &\underset{\boldsymbol{a}_m}{\operatorname{argmin}}\ \boldsymbol{a}_m^T\boldsymbol{a}_m \\ &s.t.\quad \boldsymbol{J}_m^T(\underbrace{\boldsymbol{F}_m^0\boldsymbol{a}_m}_{\boldsymbol{f}_m}) = \boldsymbol{\tau}_h, \end{aligned} \tag{4}$$

where $\boldsymbol{a}_m \in [0\ \ 1]$ indicates the muscle activation vector and $\boldsymbol{F}_m^0$ is a constant diagonal matrix, the elements of which denote the maximum isometric forces of the corresponding muscles. The muscle force $\boldsymbol{f}_m$ is then defined as a product of $\boldsymbol{F}_m^0$ and $\boldsymbol{a}_m$, implying that muscle is considered as an ideal force generator in SO. It is apparent that by holding the constraint of (2), this optimisation tries to minimise the sum of squares of muscle activations, which is a commonly employed objective function in the related research [29, 33].

Although the estimate of $\boldsymbol{\tau}_h$ can be achieved by resorting to some effective inverse kinematics algorithms in order to calculate human arm joint angles [35], and $\boldsymbol{J}_h$ and $\boldsymbol{g}_h$ in (1), the muscle Jacobian $\boldsymbol{J}_m$ requires accurate and complete musculoskeletal model of human arm to enable the optimisation in (4). A dynamic upper limb musculoskeletal model [26] was then employed by OpenSim for this purpose to implement the static optimisation that estimates muscle forces in the offline calibration phase. This model has already been proven and validated to be effective in our previous work, where another two muscle-Jacobian-dependent properties of human arm, the endpoint stiffness [36] and joint stiffness [37, 38], were successfully estimated online by using the same model.

2.2. Machine Learning and Online Force Prediction

When we obtained the feasible solutions for muscle forces from the complex offline model, we encoded them with a GPR-based machine learning method [39]. The input training data set $\boldsymbol{X}$ was composed of measured samples of human arm joint configuration $\boldsymbol{q}_h$ and endpoint force $\boldsymbol{f}$[1], both measured by the robot sensory system (i.e. vision and force sensors). The output training data set $\boldsymbol{F}_m$ was composed of corresponding feasible solutions of muscle forces $\boldsymbol{f}_m$. The known training data composed of inputs $\boldsymbol{X} = [[\boldsymbol{q}_{h1}, \boldsymbol{f}_1], ..., [\boldsymbol{q}_{hN}, \boldsymbol{f}_N]]$ and outputs $\boldsymbol{F}_m = [\boldsymbol{f}_{m1}, ..., \boldsymbol{f}_{mN}]$, which were obtained from the musculoskeletal model through the offline optimisation in (4), were used to estimate the parameters of GPR. Number N is the size of the training data input-output pairs. For illustration, the training points in different arm configurations are shown on the graphs of Fig. 2.

The GPR that encodes the desired relation is defined as

$$\begin{bmatrix} \boldsymbol{F}_m \\ \boldsymbol{f}_{m*} \end{bmatrix} \sim \mathcal{N}\Big(0, \begin{bmatrix} \boldsymbol{K}(\boldsymbol{X}, \boldsymbol{X}) + \sigma_n^2 \boldsymbol{I} & \boldsymbol{K}(\boldsymbol{X}, \boldsymbol{x}_*) \\ \boldsymbol{K}(\boldsymbol{x}_*, \boldsymbol{X}) & \boldsymbol{K}(\boldsymbol{x}_*, \boldsymbol{x}_*) \end{bmatrix}\Big), \tag{5}$$

where $\mathcal{N}$ represents Gaussian distribution, $\boldsymbol{f}_{m*}$ is the prediction corresponding to the new input $\boldsymbol{x}_* = [\boldsymbol{q}_{h*}, \boldsymbol{f}_*]$, $\boldsymbol{X}$ and $\boldsymbol{F}_m$ are input and output values from the training data set, respectively, and σ_n is variance of noise. Matrix $\boldsymbol{K}$ represents the correlations between different inputs and its elements are composed of Gaussian kernels $\sigma_f^2 \exp[-\frac{1}{2}(\boldsymbol{x}_i - \boldsymbol{x}_j)^T \boldsymbol{W}^{-1}(\boldsymbol{x}_i - \boldsymbol{x}_j)]$, where $\boldsymbol{x}_i$ and $\boldsymbol{x}_j$ are individual samples in the training set $\boldsymbol{X}$, σ_f is variance and $\boldsymbol{W}$ is a diagonal matrix containing width parameters of Gaussians. The best prediction is the mean value of the normal distribution

$$\boldsymbol{f}_{m*} = \boldsymbol{K}(\boldsymbol{x}_*, \boldsymbol{X})[\boldsymbol{K}(\boldsymbol{X}, \boldsymbol{X}) + \sigma_n^2 \boldsymbol{I}]^{-1} \boldsymbol{F}_m. \tag{6}$$

Note that the computationally expensive term $[\boldsymbol{K}(\boldsymbol{X}, \boldsymbol{X}) + \sigma_n^2 \boldsymbol{I}]^{-1} \boldsymbol{F}_m$ is not dependent on the new input $\boldsymbol{x}_*$ and was therefore pre-calculated in order to increase the real-time efficiency. During the online phase, the new input $\boldsymbol{x}_*(t) = [\boldsymbol{q}_h(t), \boldsymbol{f}(t)]$ was updated at each sample time t. The human arm configuration was measured by the optical motion capture system, where joint angles $\boldsymbol{q}_h$ and arm Jacobian $\boldsymbol{J}_h$ were obtained by the method proposed in [40]. The force sensor mounted on the robot end-effector measured the interaction force $\boldsymbol{f}$.

2.3. Human Muscle Fatigue Model

We used (6) to estimate the muscle forces of the human arm in real-time during the online stage. The estimated forces of individual muscles were used in conjunction with a fatigue model to estimate the respective muscle fatigue. The fatigue model used in our method was based on the model proposed in [21], which operated based on the measured muscle activity. Since the relationship between muscle activity and muscle force can be linearly approximated in a certain operation range [41], in the proposed work the model is modified to include muscle forces instead of muscle activities. Other fatigue models based on the muscle force from the literature follow a similar first-order system dynamics [23].

The modified muscle fatigue model is defined as a first-order system of differential equations

$$\frac{dV_i(t)}{dt} = \begin{cases} (1 - V_i(t))\frac{f_{mi}(t)}{C_i} & \text{if } f_{mi}(t) \geq f_{th} \\ -V_i(t)\frac{R}{C_i} & \text{if } f_{mi}(t) < f_{th} \end{cases}, \tag{7}$$

where $V_i \in [0 \;\; 1]$ is the i-th muscle fatigue index, f_{mi} is the estimated muscle force from (6), C_i is a capacity parameter that determines the fatigue characteristics of a specific muscle. The parameters C are subject and muscle dependent and should be tuned individually. The higher the C is, the more effort f_m over time it takes for the fatigue to occur. The parameter R is a recovery rate, which determines the speed of fatigue reduction after the muscle is relaxed. In our experiments we used a conservative value $R = 0.5$, as in [21]. Other recovery rates can be found in literature [42]. We used the threshold f_{th} to determine when the muscle is relaxed. When the muscle force is larger than this threshold, the model is in fatigue increasing mode, otherwise it is in recovery mode.

[1]Note that, instead of the endpoint force $\boldsymbol{f}$, the joint torque $\boldsymbol{\tau}_h$ can also be used as an input of GPR. However, in that case a separate model of the human arm gravity $\boldsymbol{g}_h$ is required. The advantage of using $\boldsymbol{f}$ is that $\boldsymbol{g}_h$ is indirectly incorporated through the muscle force relationship provided by the complex offline model and is therefore learnt.

We conducted a preliminary calibration experiments to determine the values of fatigue capacity parameters C as proposed in [21]. The human subjects were instructed to produce several reference muscle forces f_m^{ref} for the amount of time T, after which the subject could not endure it anymore or felt uncomfortable. We calculated C for each reference force f_m^{ref} by

$$C = -\frac{f_m^{ref} \cdot T}{\ln(1 - 0.993)}, \tag{8}$$

where the full capacity is assumed to be reached after five time constants, i.e. $V = 0.993$. As the final estimation of fatigue capacity, we then used the mean value of C parameters obtained by (8) for different reference forces.

2.4. Selective Muscle Fatigue Management

The demand for the fatigue management in human-robot collaboration tasks usually arises when a continuous force production task of considerably long duration is required to be executed by the human partner with the assistance of the robot partner. A force production task can be formally described or defined in terms of the position and orientation of human hand. If both the position and orientation are strictly constrained in the collaboration tasks, there is no room to introduce any fatigue management strategy. However, in most cases, one of these two variables is free to be exploited to inject optimisation methods for fatigue management. Therefore, we split the fatigue management problems in the human-robot co-manipulation tasks into two representative scenarios and problem formulations.

The first scenario focuses on the situations where the orientation of human hand is constrained while the position is free to be optimised, which falls into a planning problem. In this case we want to find the optimal working position where the task can be produced for the longest time with respect to the fatigue of the considered muscles in the human arm. This scenario includes many common industrial tasks, such as: drilling or polishing a surface/object in a specific direction with a prescribed force. For example, if the human needs to polish in a surface of a stationary table or wall, the orientation is constrained and the human can only change the arm configuration with respect the to endpoint position. Note that this scenario is general and can also be applied to cases where human performs the task on its own (i.e., without the robot).

The second scenario refers to the situations where the position of human hand is constrained while the orientation is adjustable for the fatigue relief, which is actually an online adaptation problem. In this case we want the robot to adapt the task execution during the actual production process in order to alternately stress or relax different groups of muscles based on the current levels of fatigue. This scenario includes industrial tasks where the work should be performed in a specific position. For example, if the human needs to fit his/her body inside a frame of a car to execute some task with the robot, the configuration of most of the body is constrained and therefore choosing between different endpoint force directions is the only option.

For each scenario we developed a novel protocol//policy that can solve the given problem. In the first scenario, the task involves a constraint on the direction of the arm endpoint force production (i.e., interaction with an object in a specified direction) but involves no constraint on the endpoint position (except for the designated workspace). The same fatigue threshold may be reached by different involved muscles at different times, due to the different activation levels f_m or capacity parameters C (experimental analysis of this aspect is in section 3.1). To manage the human fatigue in this scenario, we propose Fatigue Management Protocol 1 (*FMP1*) that involves a search for the optimal working endpoint position, where the minimum of the endurance times of all involved muscles can be maximised, while producing a prescribed endpoint force. If the desired endpoint force changes, the optimisation has to be performed again under the new condition.

In the second scenario, the task involves a constraint on the position of the arm endpoint (e.g., obstacles in the workspace that limit the choices for the optimisation, limited workspace of collaborative robot, etc.) and involves no constraints on the orientation (i.e., assuming that the robot can rotate the object). To manage the human fatigue in this scenario, we propose Fatigue Management Protocol 2 (*FMP2*) that is based on dividing the considered muscles into groups, where the endpoint force production in a certain direction involves the coordinated activation of one group, while the other group is at rest. The method then uses this information to alternate the involvement of different muscle groups based on the estimated fatigue by changing the direction of the desired endpoint force. The human can arbitrarily change the magnitude of the endpoint force, while the fatigue model estimates the current fatigue level online.

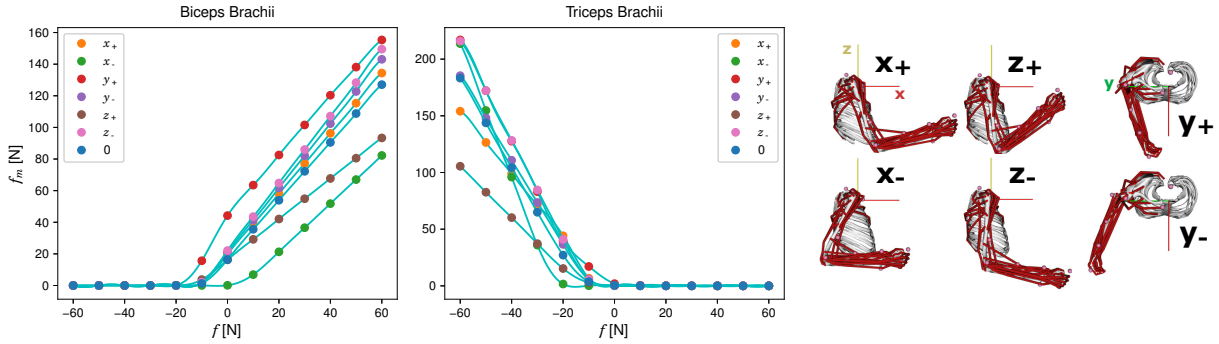

Figure 2: Results of muscle force learning. Left and right graphs display the relationship between endpoint force and muscle forces in the selected working configuration space of arm for Biceps Brachii and Triceps Brachii, respectively. The dots show the training data from the offline model, while the light blue line shows the function as learnt by GPR. Different colours of dots correspond to different arm configurations. The 0 configuration corresponds to neutral initial configuration as shown in Fig. 4E. Other configurations correspond to conditions when the endpoint was displaced along axes of the base frame for 10 cm either in positive or negative directions (see right-hand side).

2.4.1. FMP1

In this case, we use fatigue model to estimate the maximum time within which every muscle can endure under the given desired endpoint task force and fatigue parameters. The individual force of each considered muscle is estimated using the previously described machine learning technique. Deriving from the fatigue model in (7), the individual maximum endurance time for i-th muscle in a given configuration $\boldsymbol{q}_h$ and endpoint force $\boldsymbol{f}$ is defined as

$$T_i(\boldsymbol{q}_h, \boldsymbol{f}) = -\frac{C}{f_{mi}(\boldsymbol{q}_h, \boldsymbol{f})} \ln(1 - V_{th}), \tag{9}$$

where V_{th} is the specified fatigue threshold for the given muscle. Note that each muscle i can have different thresholds based on the task conditions. The individual muscle force $f_m(\boldsymbol{q}_h, \boldsymbol{f})$ is obtained from the machine learning.

The maximum endurance time of the whole arm in a given position of endpoint is equal to the minimum of maximum endurance times of all considered muscles i. Note that in different configurations there are different relationships between muscle forces and an endpoint force (see Fig. 2), and therefore the endurance time is different. The optimisation process then uses the function obtained by machine learning to find the endpoint position within the desired workspace, where the whole-arm endurance time is maximised as

$$\underset{\boldsymbol{q}_h}{\operatorname{argmax}} \left(\min_i \left(T_i(\boldsymbol{q}_h, \boldsymbol{f}) \right) \right), \tag{10}$$

Note that $\boldsymbol{q}_h$ is constrained by the joint limits and/or desired endpoint workspace, while $\boldsymbol{f}$ is constrained by the desired task.

2.4.2. FMP2

The muscle groups are determined by observing how the activation pattern of an ensemble of muscles varies as the direction of the external endpoint force changes (for an example, see Fig. 3). First, the interested muscles are divided into two candidate groups through all the possible combinations. This consideration is to divide the involved muscles into two possibly antagonistic groups, so that the task production can be switched among them. For each candidate division, we determine the overlap of activation ranges of muscles of each group in different endpoint force directions. If the overlap is large, the given combination of muscles has a strong mutual function and these muscles are considered to be more likely part of a coherent group. Then we check how much the activity ranges of both candidate groups are overlapping each other. If they do not considerably overlap, then we consider the two groups to have a good antagonistic function and should be more suitable for the proposed fatigue management based on the alternation of activity/rest phases of the two groups. The reward function for finding the most suitable combination of muscles

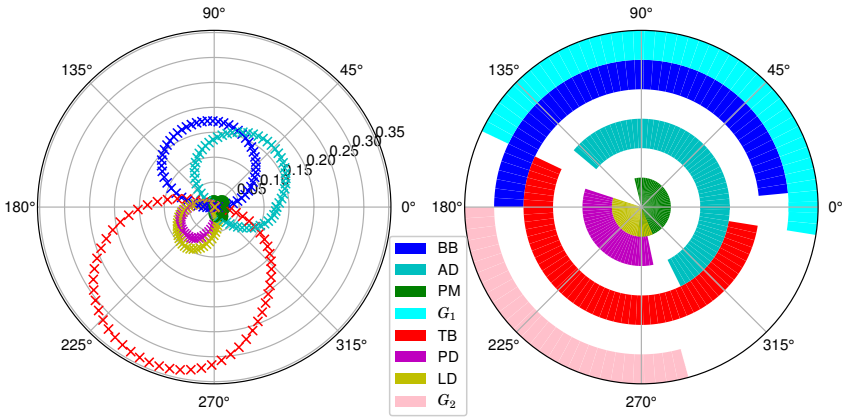

Figure 3: Results of the muscle group assignment. The left graph shows the individual muscle forces with respect to the direction of endpoint force (with the desired magnitude of 40N in this case). 0° means the endpoint force is produced in anterior direction and 90° means the endpoint force is produced in upward direction of the human arm base frame (see the right image in Fig. 4). The muscle forces are normalised to their maximum values. The right graph shows the range of activity of each muscle as described by (13). The outermost rings show the ranges of two muscle groups suitable for fatigue management as described by (14). Six dominant muscles are considered: Biceps Brachii (BB), Triceps Brachii (TB), Anterior and Posterior Deltoid (AD and PD), Pectoralis Major (PM) and Latissimus Dorsi (LD). The proposed method assigned BB, AD and PM into G_1 and TB, PD and LD into G_2.

for the two candidate groups is defined as

$$\gamma = \min\Big(\sum_{+} \boldsymbol{c}_1, \sum_{+} \boldsymbol{c}_2\Big) \cdot \sum_{+} (\boldsymbol{c}_1 \oplus \boldsymbol{c}_2), \tag{11}$$

$$\boldsymbol{c}_j = \sum_{\wedge} \boldsymbol{a}_{ji}(\boldsymbol{\phi}), \tag{12}$$

where $\boldsymbol{a}(\boldsymbol{\phi})$ is a vector that contains muscle activation levels in different endpoint force directions $\boldsymbol{\phi}$, index i denotes muscle, and index j signifies candidate group. The elements in the vector $\boldsymbol{c}_1$ reflect the overlapping activity states of the first group of muscles in different endpoint force directions, $\boldsymbol{c}_2$ is the same for the second group of muscles, $\wedge$ and $\oplus$ stand for logic AND and XOR operations, respectively. The operator $\sum_{+}$ calculates the sum of all elements in a vector and returns a scalar value, while the operator $\sum_{\wedge}$ represents a bitwise AND operation across all activation vectors $\boldsymbol{a}_i$ and returns a vector.

Note that the algorithm goes through all possible divisions of muscle groups and selects the two groups with the highest reward, i.e., $\max(\gamma)$. The left part of the product in (11) provides the information about the coherency of muscle functions in either group under a given division of muscles, i.e., how well the muscles in each group act in a coordinated manner. For example, if the muscle within the candidate group have a large overlap in the activation in different endpoint force directions, then it means that their coherency is good. The right part of the product in (11) provides the information about how well the two given candidate groups of muscles act antagonistically. For example, if the two groups of muscles do not have a large overlap in activation, then they can be considered more antagonistic.

When more than two muscles per group are considered to calculate $\boldsymbol{c}$ in (12), AND operation is performed among muscle activity vectors $\boldsymbol{a}$ of all muscles within the group. In addition, in certain combinations, a group includes only one muscle and therefore $\boldsymbol{c}_j = \boldsymbol{a}_{ji}$. The activation or inactivation is determined by the fatigue/recuperation stages and is defined as

$$a(\phi) = \begin{cases} 1 & \text{if } f_m(\boldsymbol{q}_h, f, \phi) \geq f_{th} \\ 0 & \text{if } f_m(\boldsymbol{q}_h, f, \phi) < f_{th} \end{cases}, \tag{13}$$

where the muscle force f_m depends on the joint configuration $\boldsymbol{q}_h$, magnitude of endpoint force f and its direction ϕ.

In the example presented in Fig. 3, the method assigned BB, AD and PM muscles to the first group, and TB, PD and LD muscles to the second group, since this particular combination yielded the highest reward γ.

After the two distinctive groups are defined by the above-mentioned method, the task of the fatigue management method is to find a feasible range of endpoint force production directions for each group of muscles, so that the other group is inactive (i.e., in rest). The proposed approach is defined as

$$\begin{aligned} \boldsymbol{G}_1(\boldsymbol{\phi}) &= \boldsymbol{o}_1 \wedge (\neg \boldsymbol{o}_2), \\ \boldsymbol{G}_2(\boldsymbol{\phi}) &= \boldsymbol{o}_2 \wedge (\neg \boldsymbol{o}_1), \\ \boldsymbol{o}_j &= \sum_{\vee} \boldsymbol{a}_{ji}(\boldsymbol{\phi}), \end{aligned} \tag{14}$$

where $\boldsymbol{o}_j$ is the activation range of the j-th group of muscles and $\neg \boldsymbol{o}_j$ is inactive range obtained by bitwise negation $\neg$. The operator $\sum_{\vee}$ represents a bitwise OR operation across all activation vectors $\boldsymbol{a}_i$ and returns a vector. For example, the feasible activation range of the first group $\boldsymbol{G}_1$ is equal to the subset of directions where one or more muscles from the first group is/are active and at the same time none of the muscles from the second group is active. This enables the muscles of the second group to relax anywhere inside the endpoint force angle range $\boldsymbol{G}_1$, in which the first group is active. The opposite is true for range $\boldsymbol{G}_2$. See the right graph of Fig. 3 for details.

Giving a range of endpoint force directions, instead of one single direction, enables more options for different applications and users. For example, if there are some limitations in task production (e.g., obstacles, human or robot joint limits, etc.) that may eliminate a part of the range, there can still be some other part of the range left, where the force can be produced. Note that choosing different directions within the specified range yields different muscle activity conditions (see the left graph of Fig. 3). For example, in some directions one muscle may be more active than the other muscles in that group. In a specific task example that was considered in the experiments in section 3.2, we selected the direction within the given range of directions based on the limitations of the human and the robot joint limits.

When the human is collaboratively performing a co-manipulation task, the muscle forces are obtained by the learnt GPR and the robot uses (7) to estimate the fatigue of specific muscles. When any of the muscles in the currently active group reaches the predefined threshold V_{th}, the proposed method uses (14) to make the robot change the task frame orientation in Cartesian space in order to remove the tired group of muscles from the desired endpoint force production, and consequently involves the relaxed group of muscles.

2.5. Robot Controller

We used Cartesian impedance controller to govern the robot interactive behaviour as

$$\boldsymbol{f} = \boldsymbol{K}_r(\boldsymbol{x}_a - \boldsymbol{x}_d) + \boldsymbol{D}_r(\dot{\boldsymbol{x}}_a - \dot{\boldsymbol{x}}_d), \tag{15}$$

where $\boldsymbol{f}$ is the end-effector force acting from the environment on the robot, $\boldsymbol{x}_a$ and $\boldsymbol{x}_d$ are actual and desired end-effector pose, respectively, $\boldsymbol{K}_r$ is Cartesian stiffness matrix and $\boldsymbol{D}_r$ is Cartesian damping matrix, which is obtained by *double diagonalisation design* [43]. When the robot interacts with the human, the force $\boldsymbol{f}$ in (15) corresponds to the force at the human arm endpoint from (3).

The interaction force produced by the human $\boldsymbol{f}$ was included in the control of robot dynamics as

$$\boldsymbol{M}_r(\boldsymbol{q})\ddot{\boldsymbol{q}}_r + \boldsymbol{C}_r(\boldsymbol{q}_r, \dot{\boldsymbol{q}}_r)\dot{\boldsymbol{q}}_r + \boldsymbol{g}_r(\boldsymbol{q}_r) = \boldsymbol{\tau}_r + \boldsymbol{J}_r^T(\boldsymbol{q}_r)\boldsymbol{f}, \tag{16}$$

where $\boldsymbol{\tau}_r$ is a vector of robot joint torques, $\boldsymbol{q}_r$ is vector of robot joint angles, $\boldsymbol{J}_r$ is the robot arm Jacobian matrix, $\boldsymbol{M}_r$ is inertial matrix, $\boldsymbol{C}_r$ is Coriolis and centrifugal matrix and $\boldsymbol{g}_r$ is gravity vector.

3. Experiments

The experiments included two tasks; the first was related to *FMP1* and the second was related to *FMP2*. The objective of the first task was to polish a surface of an object held by the collaborative robot. By using the proposed method, the robot found a position in Cartesian space where the human could perform this task the longest, considering the fatigue in the arm muscles. The objective of the second task was to perform drilling into an object held by the robot. The robot monitored the fatigue of the human muscles and switched the configuration of task production

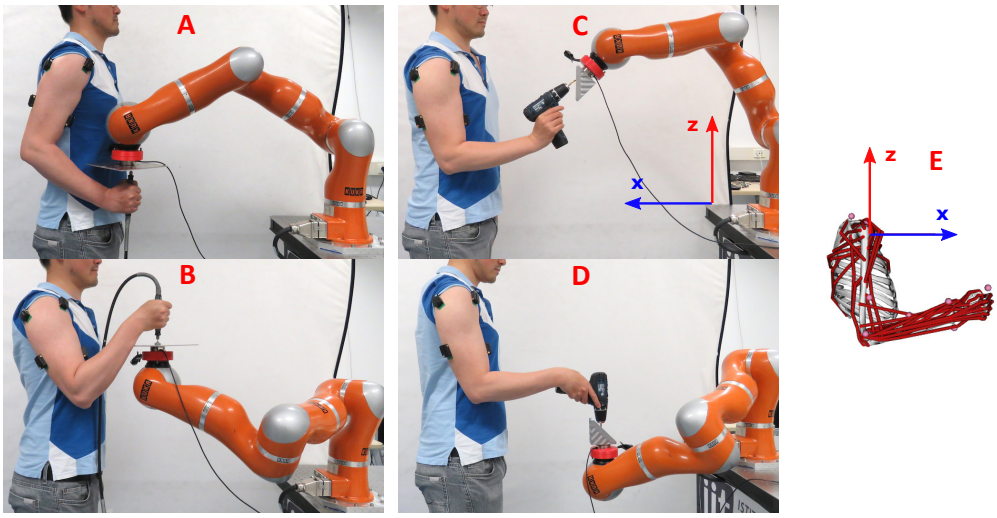

Figure 4: Illustration of experimental setup for human-robot collaborative object polishing (left column photos) and object drilling (middle column). The photo A shows the optimised polishing position for the case when the desired force direction is pointing upward. The photo B shows the optimised polishing position for the case when the desired force direction is pointing downward. The photo C shows the drilling task in the case where the first group of muscles G_1 is involved and the second group G_2 is relaxed. The photo D shows the condition after the robot changed the working configuration and therefore G_1 is relaxed and G_2 is active. The model of the human arm in the neutral initial position (as in photos C and D) from OpenSim is shown in the photo E. The two frames represent the robot arm base frame (left) and the human arm base frame (right).

to alternate between the active and relaxed modes of the predefined muscle groups and made sure that the human coworker was in a good condition.

Six male subjects participated in the experiments, who gave their informed consent. The study was approved by the Regional Ethics Committee of Liguria (IIT_HRII_001, 108/2018).

3.1. FMP1

In this scenario, there was a constraint on the direction of the endpoint force required to complete the task. Such constraint may arise due to the various working conditions and task specifics that are present in real-world setting. For this demonstration experiment, we show two force directions; one is polishing vertically upward and the other is polishing in the same axis in the opposite direction (i.e., downward). See also photos A and B in Fig. 4 for illustration. The reference force for both cases was 40 N.

The results of the upward force direction are shown in Fig. 5. The left four graphs show the muscle activity for four considered muscles[2] in different endpoint positions of Cartesian space. Since the force was pointing upward, BB and AD were activated, while TB and PD were mostly at rest throughout the selected workspace. The graph on the right side shows the estimated maximum endurance time of the arm in different endpoint positions of Cartesian space based on the considered muscles. Using (9) and (10), the robot calculated the optimal position where the endurance time was maximised (28.6 seconds). In this particular case, the optimal position was ($x = -0.1, z = -0.2$). This can also be confirmed by observing the left graph of Fig. 5.

To show that different desired polishing force direction yields different results, we performed a supplementary experiment where the force direction was reversed. The results of this experiment are shown in Fig. 6. It is clear from the graphs on the left side that muscle activity is different in comparison to Fig. 5. This is because the force is pointing downward and therefore TB and PD had to be activated, while BB and AD were mostly at rest throughout the selected workspace. Using (9) and (10), the robot calculated the optimal position where the endurance time was maximised (907.0 seconds), which was in this particular case at ($x = -0.05, z = 0.2$). Note that the endurance time is much higher in this case, which can be primarily attributed to the gravity assisting the endpoint force production in downward direction.

[2]For this demonstration experiment we used BB, TB, AD and PD muscles. Note that considering different muscles or more of them would change the result.

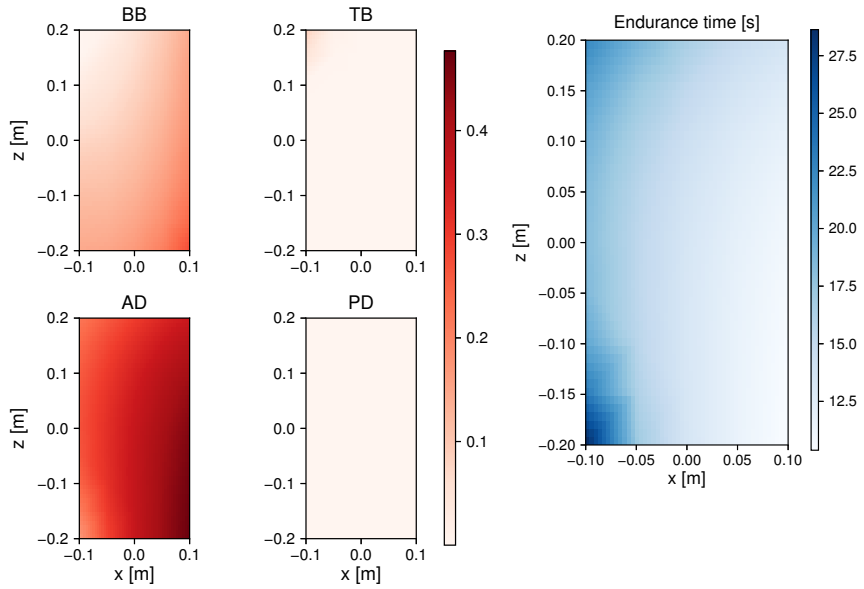

(a) Muscle activation (b) Endurance time

Figure 5: Results of the first experiment (upward endpoint force direction for polishing task). The graphs on the left side show the muscle activation (normalised to maximum force value) when producing the desired endpoint force in different positions of arm endpoint. The graph on the right side shows the endurance time (in seconds) for producing the desired endpoint force in different positions of arm endpoint. The position of arm endpoint (0,0) corresponds to configuration shown on the right photo of Fig. 4.

3.2. FMP2

The second experimental task was a collaborative human-robot object drilling (see photos C and D Fig. 4). In this scenario, there was a constraint on the endpoint position of the task production. While this constraint can be dictated by various working conditions and task specifics (e.g., obstacles in workspace, etc.), for this demonstration experiment we selected the position constraint as a neutral position based on the minimisation of overloading joint torques and maximisation of endpoint manipulability [19].

As a part of the second experiment, the human applied the force perpendicularly to the object surface in order to perform the drilling action. The reference force was 40 N. Initially, the object surface was rotated in a way that the human had to produce the endpoint force at an angle of 45° with respect to the horizontal axis in the sagittal plane (see Fig. 3 and Fig. 4C for details). When the robot detected a certain level of muscle fatigue in the human arm, it had to reconfigure the object in a way that the other group of muscles (e.g. antagonistic) were active, while the currently tired group of muscles could relax. This was done according to *FMP2*, as explained in section 2.4.2.

The main results of the second experiment for one subject are shown in Fig. 7. In the first graph we can see how the human maintained the reference endpoint force required for the drilling action. The photo C in Fig. 4 illustrates this initial configuration of task production. When the human was producing the endpoint task force, the muscles from the first group G_1 were active, as it can be confirmed by observing the second and fourth graphs. Note that the EMG measurements in the fourth graph are not necessary for method operation, but are merely presented as an additional validation.

While the muscles were active, their estimated fatigue gradually increased (see the fifth graph). At the point when the fatigue of any of the G_1 muscles reached a predefined threshold (in this case AD reached first), the robot used *FMP2* to change the configuration. By doing so the involvement of the tired group of muscles in the desired task production was minimised. In these experiments we set the fatigue threshold to 70 %[3]. The bottom graph shows how the robot changed its endpoint configuration in order to facilitate a new configuration of the drilled object. For further illustration, see photo D in Fig. 4 that shows the actual experimental setup.

[3]Note that this threshold can be selected based on the task specifics and desired working conditions.

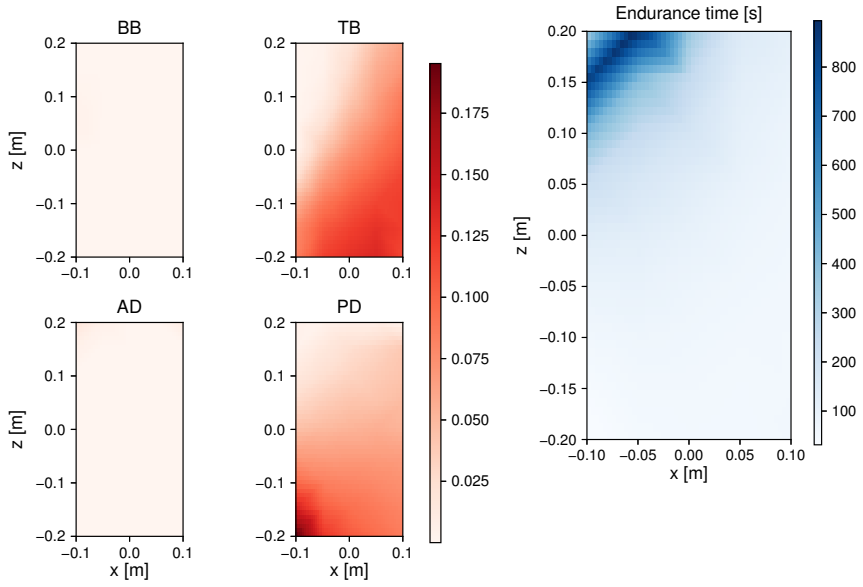

(a) Muscle activation (b) Endurance time

Figure 6: Results of the first experiment (downward endpoint force direction for polishing task). The graphs show the same variables as those in Fig. 5 under different desired endpoint force.

After the robot changed the configuration of the object, the direction of drilling force was changed. The new task force was rotated by -90°[4] with respect to the horizontal axis in the sagittal plane (see Fig. 3 and Fig. 4D for details). While the initial and new directions are not exactly opposite, we distinguish them in the first graph of Fig. 7 by a negative force sign. The effect of the new condition can be observed in the second graph, where the muscle activity of the first group G_1 decreased. In turn, the muscles of the second group G_2 took over the task force production and therefore their activity increased, as it can be observed in the third and the fourth graph.

In this experiment, the muscle force threshold that determines the relaxation mode was set to 0.02% of MVC for all muscles[5]. The relaxation phase of the first group of muscles G_1 can be observed in the fifth graph, where we can see how the fatigue levels gradually decreased. On the other hand, the estimated fatigue levels of the second group of muscles G_2 gradually increased as a result of their increased activity. When one of the muscles of G_2 reaches the predefined fatigue threshold, the load can be again redistributed to the muscles of G_1 and the process can repeat.

To show the variation of different selection of force direction within the obtained feasible range (illustrated by Fig. 3), we conducted an additional experiment where the initial drilling direction was changed from 45° to 135°. The results of this experiment are shown in Fig. 8. If we compare the muscle activations of G_1 between Fig. 7 and Fig. 8, we can see that more load was redistributed from AD to BB. Consequently, in this case BB reached the fatigue threshold first, as it can be observed in the fourth graph.

To validate the method from a quantitative perspective we conducted experiments on multiple subjects. The experimental task was the same as above. The subjects started to produce the reference force in the initial working configuration (45°). When the robot detected that the fatigue of any muscle in the first group G_1 reached the predefined threshold (70 %), the robot reacted by changing the working configuration to -90°. In the new configuration the first group of muscles G_1 could relax and the second group G_2 became active.

The results of multi-subject experiments are shown in Fig. 9. Initially, the majority of the task load was on BB and AD muscles that belong the first group G_1. When the fatigue reached the threshold, the robot altered the working configuration in order to put the tired group of muscles to rest. We can see that on average the activity of the first group of muscles G_1 was reduced when the robot changed the working configuration (comparison between the first

[4]We selected this direction among the given range of directions by considering the human and the robot joint limits. Note that the robot could select any other direction that is within the given range and that satisfies the human and the robot joint limits.

[5]Note that different thresholds can be used based on a specific application.

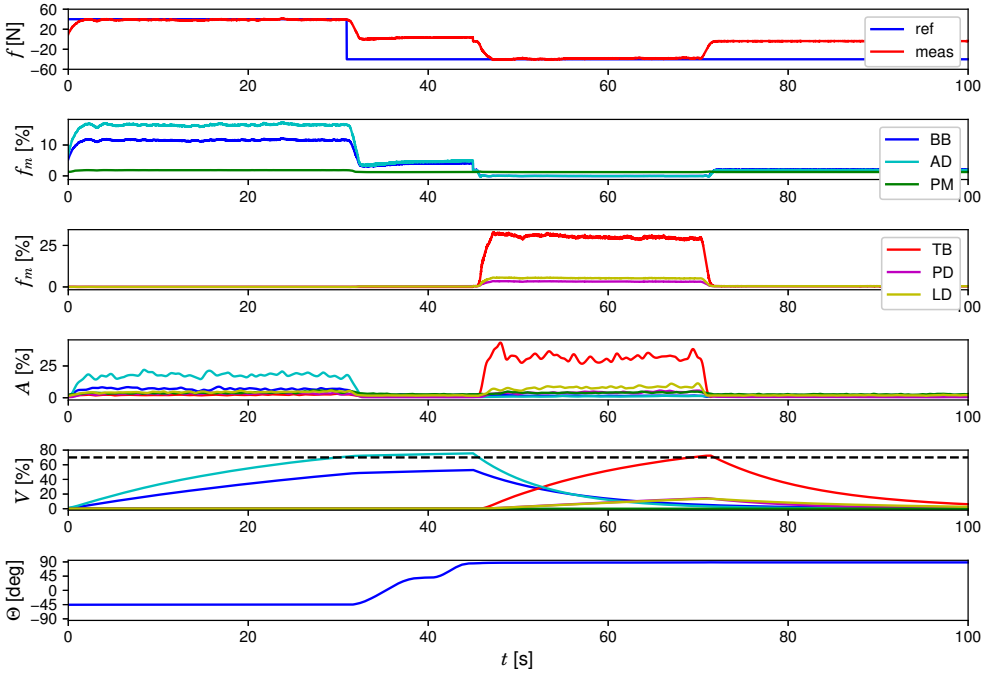

Figure 7: Results of the second experiment (drilling task) for the initial angle 45°. The first graph shows the desired (blue) and measured (red) endpoint force. The estimated muscle forces (normalised to their maximum values) for the first group G_1 (BB, AD and PM) are shown in the second graph, while forces for the second group G_2 (TB, PD, LD) are shown in the third graph. The muscle activity signals as measured by EMG are shown in the fourth graph. Note that the EMG measurement is not required for method operation and is presented only as an additional validation. The estimated fatigue level for each muscle is shown in the fifth graph. The bottom graph shows the direction of endpoint force applied by the robot in the robot base frame that is shown in Fig. 4, where the angle is in x-z plane. The angle -90° is when the robot endpoint points downward and 90° is when it points upward (both along z-axis).

and the second stage). On the other hand, the activity of the second group of muscles G_2 increased after the transition. In particular, TB muscle took over the majority of the task load[6]. This reduction/increase of muscle activity pattern was observed for all subjects. This confirms our hypothesis that the robot was able to offload the tired group and involve the group of muscles that was previously resting.

To further validate the hypothesis, we conducted a comparison study between the case when our method was used by the robot to selectively offload the tired muscle group, and the case when the robot did not use the method. To do so, each subject performed an additional experiment, where the robot did not change the working configuration. For the sake of comparison, the subjects had to produce the task without the method in the initial configuration for the same amount of time as they produced it with the method in both configurations [7]. Note that the transition time, when the robot was performing a reconfiguration trajectory, was deduced in order to make it fair. As a part of subjective evaluation, after the experiments each subject had to answer the following questions:

1. After stopping the task execution in case when the fatigue was NOT managed, I felt my arm muscles were tired.
2. After stopping the task execution in case when the robot managed the fatigue, I felt my arm muscles were LESS tired.
3. Overall, I prefer the case when the fatigue was managed by the robot.
4. The fatigue management method is useful for producing repetitive or sustained application of forces in common industrial tasks.

[6]Note that by selecting a different configuration (i.e., endpoint force direction), the robot could involve PD and LD more. However, considering this particular task and tool, there was a limitation on human wrist rotation (i.e., ulnar deviation was close to the physical limit).

[7]The experiment time was equal to the sum of endurance times of the first stage and the second stage, and the transition time required for the robot to change the configuration. For example, the considered experimental time in Fig. 7 would be 69 seconds, while the transition time is the part between the 30th second and the 45th second. Since endurance times of muscles are subject dependent, the experiment time also varied among the subjects.

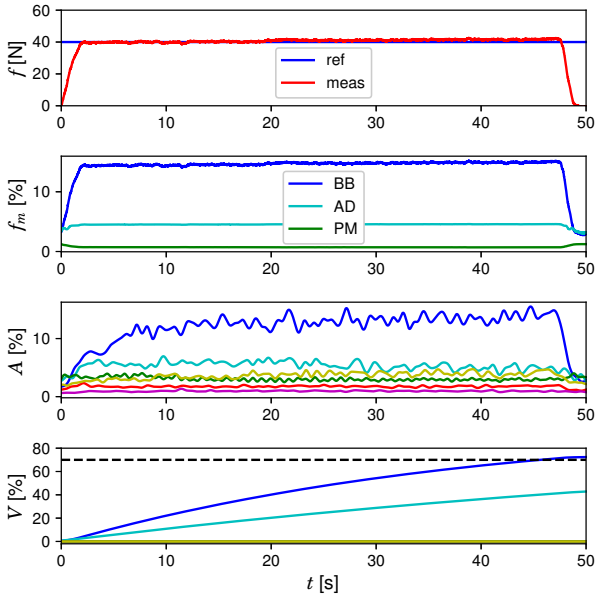

Figure 8: Results of the second experiment (drilling task) for initial angle 135°. The first graph shows the endpoint force. The second graph shows the estimated muscle forces of the first group G_1. The EMG-based muscle activity is shown in the third graph. The bottom graph shows the estimated muscle fatigue.

The possible answers (scores) were: strongly agree (2), agree (1), neutral (0), disagree (-1) and strongly disagree (-2).

The results of the multi-subject subjective evaluation are shown in Fig. 10. As expected, all subjects agreed that their arm muscles were less tired when the proposed method managed the fatigue. In addition, they preferred to perform the task in the case when the robot managed the fatigue. The subjects also generally agreed that the proposed method would be useful for producing repetitive or sustained application of forces in common industrial tasks. The results of subjective evaluation further supports the hypothesis that proposed method is able to manage the fatigue in a way that the tired muscles are put to rest and the relaxed muscles are involved in the task production instead.

4. Discussion

To demonstrate the applicability of the proposed method, we performed experiments on two industrial tasks: polishing and drilling. The method provides two protocols that can be used in both planning and online adaptation. While planning is essential in large-scale production processes, online adaptation is crucial in flexible and reconfigurable production processes involving human-robot collaboration. The safety and well-being of the human coworker is the most important aspect of such collaborative process, therefore our method provides a solution to manage the human muscle fatigue. Minimising and keeping the muscle fatigue within the desired limits contribute to ergonomic working conditions of the human and can potentially prevent productivity degradation due to excessive physical fatigue or injuries.

The subjects assessed the method overall in a very favourable manner (see Fig. 10). However, some subjects put only ”agree” instead of ”strongly agree” to question 3 and question 4. In case of question 3, the subject reported that he felt felt strong enough to do it in both cases, but still agreed that the case with the proposed method took much less effort. In case of question 4, some subjects felt that they do not have enough experience with the industrial processes and therefore only agreed.

One of the main advantages of the proposed method is that all the measurements can be performed by the sensory systems on the robot side, which can significantly increase its application in the industrial and other real-world settings. The interaction force can be measured by a force sensor mounted on the robot arm, while human kinematics can be measured by the robot’s vision system. It is fair to note that in this study we employed an expensive motion capture system that required to put optical markers on the human body. However, this system can easily be replaced by more

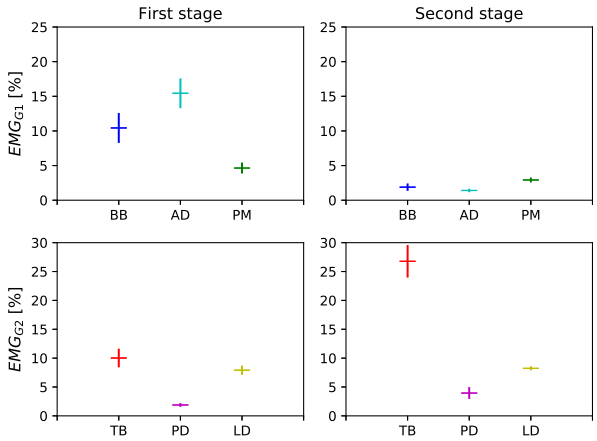

Figure 9: Results of multi-subject experiments. The graphs in the first column show the mean measured muscle activity for the initial configuration (first stage), while the graphs in the second column show the activity for the altered configuration (second stage). The vertical lines represent the standard error of mean. The first row shows the muscle activity of the first group of muscles, while the second row shows the muscle activity of the second group of muscles.

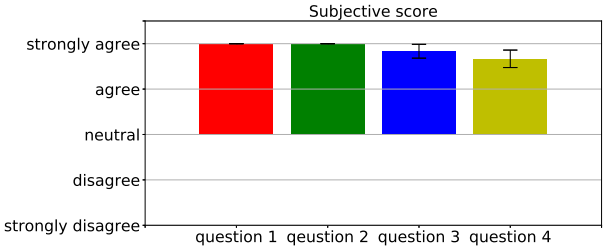

Figure 10: Results of multi-subject subjective evaluation. The bars indicate mean subjective scores given by the subjects. The black lines indicate standard error of mean.

affordable robot vision systems that can extract the limb configuration without any sensors on the human body (e.g., MS Kinect, etc.).

Unlike ad-hoc methods [20], which assume that the external force is entirely attributed to the observed muscle force, the proposed muscle force estimation method uses complex modelling, which separates the contributions of individual muscles. While taking the advantage of the complex offline modelling methods, the prediction of the individual muscle force is performed online. This property is essential in estimation of the human fatigue in real-time. On the other hand, compared to methods that use EMG sensors to measure the fatigue of individual muscles [21], the proposed method does not require any sensors on the human arm. Another advantage over the online EMG-based fatigue estimation method is that the proposed method can estimate force of muscles that lay deeper in the body and are difficult to reach by surface EMG.

A potential disadvantage of the proposed online muscle force prediction method is that it requires the training data across the workspace that dictated by the task. If the task is straightforward and is well defined, the training dataset can include a limited amount of configurations and endpoint forces. To cover the entire workspace of the arm with high amount of sampling points may be time-consuming and could slow down the real-time prediction capacity of GPR. Since GPR is a type of global regression, it considers all training data points in the calculation of prediction. An alternative is to use complimentary machine learning methods that employ local regression, such as Locally Weighted Regression [44] or Local Gaussian Process Regression [45]. However, due to the approximation of each local area with a separate model, these alternative methods tend to be less precise and therefore a tradeoff between accuracy and speed should be considered.

Another potential drawback is that the proposed muscle force and muscle fatigue model parameters are subject dependent and need to be calibrated for each human worker separately. Nevertheless, once the offline calibration process is done, the parameters can be subsequently reused in the online task production for extended periods (assuming

that the human body properties remain relatively constant).

Further potential limitations can be associated with the used hardware and working conditions. If the used hardware (e.g. optical motion capture system or vision) is not precise, the estimation of arm pose will suffer in precision and the proposed method will be affected. In addition, some working conditions may cause that something blocks the field of view of motion capture system or vision and the arm configuration might temporarily not be measured. Such conditions should be avoided in order for the proposed method to work optimally.

As we stated in section 2.4.2, the muscle division approach provides a range of possible endpoint force directions (right graph of Fig. 3), instead of one single direction. The advantage of this is that the range offers more options when considering various applications, conditions and users. For example, if we want to weight the involvement of muscles in a specific group, we can select the direction within the range, where some muscles are more active than the others (left graph of Fig. 3).

In this study we considered two main constraints of working pose: position constraint and orientation constraint. In practise, other constraints can be considered, such as, the human must see the interaction between the tool and the object. In such case, the configuration presented in Fig. 4A could not be considered from the beginning.

References

[1] A. Ajoudani, A. M. Zanchettin, S. Ivaldi, A. Albu-Schäffer, K. Kosuge, O. Khatib, Progress and prospects of the human–robot collaboration, Autonomous Robots.

[2] A. Cherubini, R. Passama, A. Crosnier, A. Lasnier, P. Fraisse, Collaborative manufacturing with physical humanrobot interaction, Robotics and Computer-Integrated Manufacturing 40 (2016) 1 – 13.

[3] E. Matsas, G.-C. Vosniakos, D. Batras, Prototyping proactive and adaptive techniques for human-robot collaboration in manufacturing using virtual reality, Robotics and Computer-Integrated Manufacturing 50 (2018) 168–180.

[4] K. Kosuge, Y. Fujisawa, T. Fukuda, Mechanical system control with man-machine-environment interactions, in: [1993] Proceedings IEEE International Conference on Robotics and Automation, 1993, pp. 239–244.

[5] R. Ikeura, H. Inooka, Variable impedance control of a robot for cooperation with a human, in: Robotics and Automation (ICRA), 1995 IEEE Intl. Conf. on, Vol. 3, 1995, pp. 3097–3102.

[6] T. Tsumugiwa, R. Yokogawa, K. Hara, Variable impedance control based on estimation of human arm stiffness for human-robot cooperative calligraphic task, in: Robotics and Automation (ICRA), 2002 IEEE Intl. Conf. on, Vol. 1, 2002, pp. 644–650.

[7] P. Evrard, E. Gribovskaya, S. Calinon, A. Billard, A. Kheddar, Teaching physical collaborative tasks: object-lifting case study with a humanoid, in: IEEE-RAS Intl. Conf. on Humanoid Robots, 2009, pp. 399–404.

[8] S. Ikemoto, H. Ben Amor, T. Minato, B. Jung, H. Ishiguro, Physical human-robot interaction: Mutual learning and adaptation, Robotics Automation Magazine, IEEE 19 (4) (2012) 24 –35.

[9] P. Donner, M. Buss, Cooperative swinging of complex pendulum-like objects: Experimental evaluation, IEEE Transactions on Robotics 32 (3) (2016) 744–753.

[10] L. Peternel, N. Tsagarakis, A. Ajoudani, A human-robot co-manipulation approach based on human sensorimotor information, IEEE Transactions on Neural Systems and Rehabilitation Engineering 25 (7) (2017) 811–822.

[11] H. Ben Amor, G. Neumann, S. Kamthe, O. Kroemer, J. Peters, Interaction primitives for human-robot cooperation tasks, in: Robotics and Automation (ICRA), 2014 IEEE Intl. Conf. on, 2014, pp. 2831–2837.

[12] D. Agravante, A. Cherubini, A. Bussy, P. Gergondet, A. Kheddar, Collaborative human-humanoid carrying using vision and haptic sensing, in: Robotics and Automation (ICRA), 2014 IEEE Intl. Conf. on, 2014, pp. 607–612.

[13] W. Kim, J. Lee, L. Peternel, N. Tsagarakis, A. Ajoudani, Anticipatory robot assistance for the prevention of human static joint overloading in human–robot collaboration, IEEE Robotics and Automation Letters 3 (1) (2018) 68–75.

[14] V. Duchaine, C. Gosselin, General model of human-robot cooperation using a novel velocity based variable impedance control, in: Eurohaptics Conference and Symposium on Haptic Interfaces for Virtual Environment and Teleoperator Systems, 2rd Joint, 2007, pp. 446–451.

[15] J. Medina, M. Shelley, D. Lee, W. Takano, S. Hirche, Towards interactive physical robotic assistance: Parameterizing motion primitives through natural language, in: RO-MAN, 2012 IEEE, 2012, pp. 1097–1102.

[16] K. Schaaff, T. Schultz, Towards an eeg-based emotion recognizer for humanoid robots, in: Robot and Human Interactive Communication, 2009. RO-MAN 2009. The 18th IEEE International Symposium on, IEEE, 2009, pp. 792–796.

[17] N. Nikolakis, V. Maratos, S. Makris, A cyber physical system (cps) approach for safe human-robot collaboration in a shared workplace, Robotics and Computer-Integrated Manufacturing 56 (2019) 233–243.

[18] L. Bascetta, G. Ferretti, Ensuring safety in hands-on control through stability analysis of the human-robot interaction, Robotics and Computer-Integrated Manufacturing 57 (2019) 197–212.

[19] L. Peternel, W. Kim, J. Babič, A. Ajoudani, Towards ergonomic control of human-robot co-manipulation and handover, in: 2017 IEEE-RAS 17th International Conference on Humanoid Robotics (Humanoids), 2017, pp. 55–60.

[20] B. Sadrfaridpour, H. Saeidi, J. Burke, K. Madathil, Y. Wang, Modeling and Control of Trust in Human-Robot Collaborative Manufacturing, Springer US, Boston, MA, 2016, pp. 115–141.

[21] L. Peternel, N. Tsagarakis, D. Caldwell, A. Ajoudani, Robot adaptation to human physical fatigue in human–robot co-manipulation, Autonomous Robots 42 (5) (2018) 1011–1021.

[22] C. J. De Luca, Myoelectrical manifestations of localized muscular fatigue in humans., Critical reviews in biomedical engineering 11 (4) (1984) 251–279.

[23] L. Ma, D. Chablat, F. Bennis, W. Zhang, A new simple dynamic muscle fatigue model and its validation, Intl. Journal of Industrial Ergonomics 39 (1) (2009) 211 – 220.
[24] M. Millard, T. Uchida, A. Seth, S. L. Delp, Flexing computational muscle: modeling and simulation of musculotendon dynamics, Journal of biomechanical engineering 135 (2) (2013) 021005.
[25] M. Damsgaard, J. Rasmussen, S. T. Christensen, E. Surma, M. de Zee, Analysis of musculoskeletal systems in the anybody modeling system, Simulation Modelling Practice and Theory 14 (8) (2006) 1100 – 1111.
[26] K. R. Saul, X. Hu, C. M. Goehler, M. E. Vidt, M. Daly, A. Velisar, W. M. Murray, Benchmarking of dynamic simulation predictions in two software platforms using an upper limb musculoskeletal model, Computer methods in biomechanics and biomedical engineering 18 (13) (2015) 1445–1458.
[27] L. Peternel, C. Fang, N. Tsagarakis, A. Ajoudani, Online human muscle force estimation for fatigue management in human-robot co-manipulation, in: Intelligent Robots and Systems (IROS), 2016 IEEE/RSJ Intl. Conf. on, 2018, pp. 1340–1346.
[28] M. Turvey, Action and perception at the level of synergies, Human Movement Science 26 (4) (2007) 657–697.
[29] A. Erdemir, S. McLean, W. Herzog, A. J. van den Bogert, Model-based estimation of muscle forces exerted during movements, Clinical biomechanics 22 (2) (2007) 131–154.
[30] D. G. Thelen, F. C. Anderson, S. L. Delp, Generating dynamic simulations of movement using computed muscle control, Journal of biomechanics 36 (3) (2003) 321–328.
[31] A. Seth, M. G. Pandy, A neuromusculoskeletal tracking method for estimating individual muscle forces in human movement, Journal of biomechanics 40 (2) (2007) 356–366.
[32] F. C. Anderson, M. G. Pandy, Dynamic optimization of human walking, Journal of biomechanical engineering 123 (5) (2001) 381–390.
[33] F. C. Anderson, M. G. Pandy, Static and dynamic optimization solutions for gait are practically equivalent, Journal of biomechanics 34 (2) (2001) 153–161.
[34] Y.-C. Lin, T. W. Dorn, A. G. Schache, M. G. Pandy, Comparison of different methods for estimating muscle forces in human movement, Proceedings of the Institution of Mechanical Engineers, Part H: Journal of Engineering in Medicine 226 (2) (2012) 103–112.
[35] C. Fang, A. Ajoudani, A. Bicchi, N. Tsagarakis, A real-time identification and tracking method for the musculoskeletal model of human arm, in: Systems, Man, and Cybernetics (SMC), 2018 IEEE International Conference on, 2018, pp. 3462–3469.
[36] A. Ajoudani, C. Fang, N. Tsagarakis, A. Bicchi, Reduced-complexity representation of the human arm active endpoint stiffness for supervisory control of remote manipulation, The International Journal of Robotics Research 37 (1) (2018) 155–167.
[37] C. Fang, A. Ajoudani, A. Bicchi, N. G. Tsagarakis, Online model based estimation of complete joint stiffness of human arm, IEEE Robotics and Automation Letters 3 (1) (2018) 84–91.
[38] C. Fang, G. F. Rigano, N. Kashiri, A. Ajoudani, J. Lee, N. G. Tsagarakis, Online joint stiffness transfer from human arm to anthropomorphic arm, in: Systems, Man, and Cybernetics (SMC), 2018 IEEE International Conference on, 2018, pp. 1453–1460.
[39] C. E. Rasmussen, C. K. Williams, Gaussian process for machine learning, MIT press, 2006.
[40] X. Ding, C. Fang, A novel method of motion planning for an anthropomorphic arm based on movement primitives, IEEE/ASME Transactions on Mechatronics 18 (2) (2013) 624–636.
[41] N. Hogan, Adaptive control of mechanical impedance by coactivation of antagonist muscles, Automatic Control, IEEE Transactions on 29 (8) (1984) 681–690.
[42] L. Ma, D. Chablat, F. Bennis, W. Zhang, F. Guillaume, A new muscle fatigue and recovery model and its ergonomics application in human simulation, Virtual and Physical Prototyping 5 (3) (2010) 123–137.
[43] A. Albu-Schäffer, C. Ott, U. Frese, G. Hirzinger, Cartesian impedance control of redundant robots: recent results with the DLR-light-weight-arms, in: Robotics and Automation (ICRA), 2003 IEEE Intl. Conf. on, Vol. 3, 2003, pp. 3704–3709.
[44] S. Schaal, C. G. Atkeson, Constructive incremental learning from only local information, Neural Comput. 10 (8) (1998) 2047–2084.
[45] D. Nguyen-Tuong, J. Peters, Local gaussian process regression for real-time model-based robot control, in: Intelligent Robots and Systems (IROS), 2008 IEEE/RSJ International Conference on, 2008, pp. 380–385.